

JPP 2011, 63: 918–925

© 2011 The Authors

JPP © 2011 Royal

Pharmaceutical Society

Received September 25, 2010

Accepted April 11, 2011

DOI

10.1111/j.2042-7158.2011.01296.x

ISSN 0022-3573

Metronidazole leads to enhanced uptake of imatinib in brain, liver and kidney without affecting its plasma pharmacokinetics in mice

Shin Yee Tan, Elaine Kan, Wei Yin Lim, Grace Chay,
Jason H. K. Law, Gian Wan Soo, Nadeem Irfan Bukhari and
Ignacio Segarra

Department of Pharmaceutical Technology, School of Pharmacy and Health Sciences, International Medical University, Kuala Lumpur, Malaysia

Abstract

Objectives The pharmacokinetic interaction between metronidazole, an antibiotic–antiparasitic drug used to treat anaerobic bacterial and protozoal infections, and imatinib, a CYP3A4, P-glycoprotein substrate kinase inhibitor anticancer drug, was evaluated.

Methods Male imprinting control region mice were given 50 mg/kg imatinib PO (control group) or 50 mg/kg imatinib PO, 15 min after 40 mg/kg PO metronidazole (study group). Imatinib plasma, brain, kidney and liver concentrations were measured by HPLC and non-compartmental pharmacokinetic parameters estimated.

Key findings Metronidazole coadministration resulted in a double-peak imatinib disposition profile. The maximum concentration (C_{max}) decreased by 38%, the area under the curve ($AUC_{0-\infty}$) decreased by 14% and the time to C_{max} (T_{max}) was earlier (50%) in plasma. Apparent volume of distribution (V_{ss}/F) and oral clearance (Cl/F) increased by 21% and 17%, respectively. Imatinib tissue penetration was higher after metronidazole coadministration, with 1.7 and 2.1-fold $AUC_{0-\infty}$ increases in liver and kidney, respectively. Metronidazole increased imatinib's tissue-to-plasma $AUC_{0-\infty}$ ratio in liver from 2.29 to 4.53 and in kidney from 3.04 to 7.57, suggesting higher uptake efficiency. Brain C_{max} was 3.9-fold higher than control and $AUC_{0-t_{last}}$ was 2.3-fold greater than plasma (3.5% in control group). No tissue-plasma concentration correlation was found.

Conclusions Metronidazole slightly decreased imatinib systemic exposure but enhanced liver, kidney and brain penetration, probably due to metronidazole-mediated inhibition of P-glycoprotein and other efflux transporters. The high brain exposure opens possibilities for treatment of glioma and glioblastoma. Renal and hepatic functions may need to be monitored due to potential renal and hepatic toxicity.

Keywords brain drug delivery; drug–drug interaction; imatinib; metronidazole; tissue distribution

Introduction

Drug–drug interactions are one of the main causes of therapeutic failure. These interactions can be attributed to changes in the absorption, distribution, metabolism and excretion processes that affect the pharmacokinetics and pharmacological activity of the drugs. Pharmacokinetic interactions often involve metabolising enzymes or transporters and affect the total exposure of the drugs.^[1]

Imatinib is a tyrosine kinase inhibitor that acts competitively on the ATP binding site of the platelet-derived growth factor receptor (PDGFR), the Bcr-Abl fusion protein, the tyrosine kinase receptor c-kit and the ABL-related gene protein.^[2] The specific activity on Bcr-Abl and c-kit was utilised to treat the chronic, accelerated and blast crisis phases of chronic myeloid leukaemia and gastrointestinal stromal tumours (GIST).^[2] Imatinib may also be used to treat acute lymphoblastic leukaemia, dermatofibrosarcoma protuberans, myelodysplastic/myeloproliferative diseases associated with the PDGFR gene rearrangement, advanced hypereosinophilic syndrome and chronic eosinophilic leukaemia. Additional potential therapeutic uses include renal cell carcinoma,^[3] glioma^[4] and small cell lung cancer,^[2] amongst others.

Correspondence: Ignacio Segarra, Department of Pharmaceutical Technology, School of Pharmacy and Health Sciences, International Medical University, no. 126 Jalan 19/155 B, Bukit Jalil, 57000 Kuala Lumpur, Malaysia.
E-mail: segarra100@gmail.com

Present address: Ignacio Segarra, Department of Pharmaceutics, San Jorge University, Autovia A-23 Zaragoza-Huesca Km 510, 50830 Villanueva de Gállego (Zaragoza), Spain.

In humans, imatinib is 95% bound to α -1-acid glycoprotein at therapeutic concentrations and has extensive tissue distribution.^[5] Metabolism of imatinib is mediated mainly through CYP3A4 and CYP3A5 into active metabolite N-demethylated piperazine (CGP74588), while CYP1A2, CYP2D6, CYP2C9 and CYP2C19 isoenzymes have minor involvement.^[6] Excretion of imatinib through bile is ~68% and ~13% is recovered unchanged in urine.^[5] The elimination half-life of CGP74588 (~40 h) is longer than the half-life of the parent drug (~18 h).^[5] Imatinib is a substrate and modulator of a variety of efflux transporters, which strongly affects their pharmacokinetics and has shown limited brain distribution in monkeys,^[7] mice^[8,9] and humans,^[10] due to efflux transporters at the blood–brain barrier (BBB) such as P-glycoprotein (P-gp) and breast cancer resistance protein (Bcrp).^[11] Consequently, it is anticipated that the long-term use of imatinib may lead to metastatic tumours of the central nervous system, a common site of relapse for cancer patients treated with imatinib despite its success in systemic remission.^[10] In-vitro studies have shown growth inhibition of glioma and glioblastoma cell lines, which would further support imatinib's use against malignant gliomas and meningiomas.^[12,13] However, clinical trial results have shown that imatinib monotherapy has minimal efficacy against malignant glioma.^[4] Additionally, studies in mice have shown that the chronic use of imatinib resulted in neurological deficit after 2–4 months, due to leukaemia of the central nervous system.^[14]

Imatinib is the drug of choice for GIST treatment as a neoadjuvant prior to surgery and thereafter as adjuvant therapy.^[2] Due to imatinib being a CYP3A4 and P-gp substrate, potential interactions with drugs used during postoperative infections or their prophylaxis may take place,^[1] causing pharmacokinetic and pharmacodynamic interactions.^[15]

Metronidazole is a imidazole antibiotic and antiparasitic agent used to treat anaerobic bacterial and protozoal infections. It is the first-choice antibiotic for colorectal surgical prophylaxis and postoperative complications – in combination with second- or third-generation cephalosporins.^[11] Metronidazole is rapidly absorbed (bioavailability ~90%), achieves peak plasma concentration within 1–2 h of oral administration and has low plasma protein binding (~15%).^[16] It has large tissue distribution, which achieves a cerebrospinal fluid concentration that approximates to 40% of its serum concentration.^[17] Around 90% of the metronidazole dose undergoes CYP3A4- and CYP2E1-mediated metabolism to form its major active metabolite 2-hydroxymetronidazole and the inactive 1-acetic acid metronidazole metabolite.^[18] The fraction excreted unchanged in urine is less than 10%.^[18] and glucuronidated metabolites account for 15% of the total dose eliminated.^[19] Most of the metabolites are eliminated through urine (60–80%) while 6–15% of the dose is eliminated through faeces.^[17]

Drugs that interact with metronidazole seem to cause induction or inhibition of liver microsomal enzymes, especially CYP3A4 and CYP2C9 isoenzymes. Interaction with quinidine^[20] and tacrolimus^[21] resulted in toxicity and elevated plasma concentrations, probably due to inhibitory activity on cytochrome P450 isoforms. However, contradictory findings were reported in pharmacokinetic studies with lorazepam and alprazolam.^[22] Metronidazole appears to interact with certain substrates of CYP3A but the mechanism underlying these

interactions seems not to be a result of CYP3A4/5 inhibition only.^[23] Rather it appears that metronidazole exerts its effect by inhibiting P-gp whilst sparing CYP3A enzymes.

Because of metronidazole's broad-spectrum of action, it may be used in GIST surgical treatment. Imatinib undergoes cytochrome P450 mediated metabolism, which may be inhibited by metronidazole, leading to a pharmacokinetic-based drug–drug interaction affecting the efficacy of both drugs or altering their toxicity profile.

In general, drug–drug interaction studies only assess changes in plasma/blood pharmacokinetic profiles. However, the interactions may lead to changes in the tissue distribution pattern, which can result in changes in pharmacological effect or toxicity. This study attempts to characterise the extent of the interaction, evaluating the pharmacokinetic profile and imatinib distribution to brain, liver and kidney after coadministration with metronidazole. This information will allow a better understanding of the potential benefits or risks of metronidazole coadministration to patients undergoing imatinib treatment.

Materials and Methods

Metronidazole (Sigma-Aldrich, St Louis, USA) and imatinib mesylate (Cipla Ltd, Mumbai, India), were kept refrigerated and protected from light. Methanol and acetonitrile (Merck, Darmstadt, Germany) were of HPLC grade; glacial acetic acid (Fischer Scientific, UK) and triethylamine (Nacalai Tesque Inc. Kyoto, Japan) were of analytical grade. Finally, sodium chloride was from Promega (Madison, USA), ethanol 95% from HmbG Chemicals (Hamburg, Germany) and heparin sodium from Sigma-Aldrich (Darmstadt, Germany).

The Institutional Animal Use and Ethics Committee reviewed and approved all study procedures prior to initiation of the studies. Imprinting control region (ICR) mice, male, 8–12 weeks of age, 18–25 g, were purchased from the Universiti Putra Malaysia (Kuala Lumpur, Malaysia) and kept under a 12-hour light cycle at constant temperature with water and food *ad libitum*. Mice were randomly assigned to either control or study group, and were fasted for 12 h before dosing. Mice in the control group were given 50 mg/kg of imatinib orally in ultrapure water with a 22G feeding needle (Braintree Scientific Inc., Braintree, USA) attached to a 1 ml syringe (Terumo Corp., Binan, Philippines). Mice in the study group were orally administered 40 mg/kg metronidazole in ultrapure water 15 min prior to the oral dose of imatinib (50 mg/kg). At pre-scheduled time points following imatinib administration (2, 5, 10, 20, 40 min, 1, 2, 4, 6 and 10 h) mice were euthanised by cervical dislocation ($n = 4$ per time point) and exsanguinated via cardiac puncture to remove blood in the tissues. The plasma was then separated by centrifugation (1500 rpm, 10 min, 4°C), and the brain, liver and kidneys were harvested, rinsed with 0.9% saline solution and kept at –35°C until analysis.

Sample processing and analytical assay

Imatinib concentration in plasma and tissues was measured by HPLC following a previously developed assay.^[8,24] Briefly, plasma was added to an equal volume of methanol, mixed (vortexed) and centrifuged (15 000 rpm, 15 min, 4°C), and the

supernatant transferred to HPLC microvials. The tissues were added to the extraction solvent (40% water, 30% methanol, 30% acetonitrile, pH 4.0) to reach a 10 ml/g dilution for kidneys and liver, and 4 ml/g for brain. On homogenisation (35 000 rpm), an aliquot of slurry was sonicated in an ice bath (1 min), centrifuged (15 000 rpm, 4°C, 15 min) and the supernatant transferred to a HPLC microvial for injection.

Processed plasma or tissue samples were injected (100 µl) into an Inertsil® CN-3 column (150 × 4.6 mm, 5 µm) and eluted (1 ml/min) with a pH 4.8 mixture of 1% triethylamine, 35% methanol and 74% water, and detected at 268 nm with an Agilent 1200 Series HPLC system (Agilent Technologies Inc., Santa Clara, USA). Imatinib was quantified with an external calibration curve (range of linearity 0.1 to 25 µg/ml). Imatinib recovery from plasma and tissue samples was above 75%; accuracy, and intra- and interday variability were less than 15%. The limit of quantification (LOQ) was established at 0.1 µg/ml and the detection limit was set at 0.05 µg/ml.^[24] There was no matrix interference and metronidazole did not interfere with imatinib detection. Samples with concentration below the LOQ (BLOQ) were treated as zero.

Pharmacokinetic data analysis

The pharmacokinetic parameters were calculated using non-compartmental analysis. The maximum concentration (C_{max}) and time to maximum concentration (T_{max}) were determined directly from the pharmacokinetic profiles. The elimination half-life ($t_{1/2}$) was calculated by $\ln 2/k_{el}$, where k_{el} (the elimination rate constant) was calculated from the log-linear regression of the terminal slope of the pharmacokinetic profile. The log-trapezoidal rule was used to calculate the area under the curve from time zero to the last concentration measured, $AUC_{0 \rightarrow t_{last}}$. The $AUC_{t_{last} \rightarrow \infty}$ (extrapolated AUC) was calculated as the last measured concentration divided by the elimination rate constant, C_{last}/k_{el} . Total exposure ($AUC_{0 \rightarrow \infty}$) was the addition of $AUC_{0 \rightarrow t_{last}}$ and $AUC_{t_{last} \rightarrow \infty}$. Oral clearance, Cl/F was calculated as $D/AUC_{0 \rightarrow \infty}$, where D represents the dose; the mean residence time (MRT) was calculated as $AUMC_{0 \rightarrow \infty}/AUC_{0 \rightarrow \infty}$, where $AUMC$ is the area under the first moment or the curve. Finally, the apparent volume of distribution at steady state, V_{SS}/F , was calculated as $MRT \times Cl/F$.

Statistical methods

The $AUC_{0 \rightarrow t_{last}}$ was calculated using the method developed by Bailer.^[25] This method allows the estimation of AUC from pharmacokinetic profiles generated with sparse sampling or destructive sampling, e.g. in tissue distribution studies when each experimental animal can only contribute one sample to the profile. The $AUC_{0 \rightarrow \infty}$ was calculated using a modification of Bailer's method developed by Yuan.^[26] The comparison of the AUC between the control and study groups was also performed following the methodology proposed by Bailer.^[25]

For each time point the average and standard deviation of imatinib concentration in the plasma and tissues of four mice was calculated. Comparison of each time point concentration as well as the C_{max} between the control and study groups was done using the Mann–Whitney U test and a $P \leq 0.05$ was considered significant. However, a full comparison of each time point in the brain profile could not be done due to undetectable or BLOQ levels of imatinib in the control group.

Results

The pharmacokinetic parameters of imatinib in plasma were calculated after administration of imatinib alone or after coadministration with metronidazole to mice (Table 1). The metronidazole affected the imatinib disposition profile, and plasma levels were lower in the study group than in the control group (Figure 1). The C_{max} was reduced by 38% and was reached earlier (20 min versus 40 min in the control group). In addition, the $AUC_{0 \rightarrow \infty}$ was 14% lower. However, neither the C_{max} nor the AUC showed statistical differences ($P > 0.05$) based on the Mann–Whitney U test or Bailer's method, respectively. Furthermore, a second peak appeared at 4 h in the study group and was verified with additional experiments. Calculation of the elimination rate constant (k_{el}) in the study group could only be done using the last two data points, to exclude the second peak at 4 h. Thus, the final k_{el} value (0.454 h⁻¹) is likely to be overestimated. For the control group, the calculation of

Table 1 Model independent pharmacokinetic parameters of imatinib in plasma after oral administration of 50 mg/kg alone (control group; $n = 4$ per time point) or coadministered with 40 mg/kg of metronidazole (study group; $n = 4$ per time point)

Parameter	Control group	Study group
C_{max}^a (µg/g)	6.12 ± 1.96	3.82 ± 1.64
T_{max} (min)	40	20
k_{el} (h ⁻¹)	0.293	0.454
$t_{1/2}$ (h)	2.4	1.5
$AUC_{0 \rightarrow t_{last}}^b$ (µg h/ml)	20.72 ± 0.74	18.00 ± 1.31
$AUC_{0 \rightarrow \infty}^c$ (µg h/ml)	21.49 ± 1.95	18.44 ± 2.84
MRT (h)	3.6	3.6
V_{SS}/F (L/kg)	8.10	9.77
Cl/F (L/h/kg)	2.31	2.71

^aMean ± SD. Mann–Whitney U test did not find differences in C_{max} .

^bMean ± SE, based on Bailer's method for sparse sampling.^[25]

^cMean ± SD, based on Yuan's extension of Bailer's method to infinity.^[26]

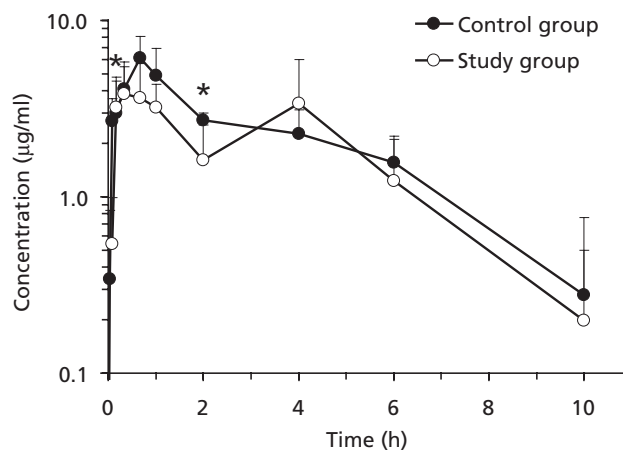


Figure 1 Plasma pharmacokinetic profile of imatinib after oral administration of 50 mg/kg (control group; $n = 4$ per time point) or coadministered with 40 mg/kg metronidazole (study group; $n = 4$ per time point) to mice. Data represent mean ± SD; *statistically different based on Mann–Whitney U test.

Table 2 Model independent pharmacokinetic parameters of imatinib in tissues after administration of 50 mg/kg alone (control group; $n = 4$ per time point) or coadministration of 40 mg/kg of metronidazole to mice (study group; $n = 4$ per time point)

Tissue	Group	C_{max} ($\mu\text{g/g}$) ^a	T_{max} (min)	k_{el} (h^{-1})	$t_{1/2}$ (h)	$AUC_{0 \rightarrow t_{last}}$ ($\mu\text{g h/g}$) ^b	$AUC_{0 \rightarrow \infty}$ ($\mu\text{g h/g}$) ^c	MRT (h)
Liver	Control	16.00 \pm 1.72	40	0.355	2.0	44.47 \pm 2.51	49.19 \pm 6.95	2.9
	Study	14.99 \pm 8.12	40	0.108	3.8	70.15 \pm 4.17***	83.61 \pm 10.45***	5.4
Kidney	Control	10.15 \pm 4.76	60	0.317	2.2	61.48 \pm 2.37	65.36 \pm 5.78	6.1
	Study	17.29 \pm 13.77	60	0.128	5.4	95.82 \pm 5.42***	139.61 \pm 14.92***	8.5
Brain	Control	1.35 \pm 1.35	20	–	–	0.72 \pm 0.15	–	4.6 ^{d,e}
	Study	5.21 \pm 3.11	2	–	–	40.57 \pm 4.69***	–	6.6 ^e

*** $P < 0.001$ based on Baileir's method for sparse sampling. ^aData are mean \pm SD for the first peak observed. Mann–Whitney U test did not find differences in C_{max} . ^bData are mean \pm SE.^[25] ^cData are mean \pm SD.^[26] ^dCould not be calculated accurately due to insufficient concentration data in brain tissue. ^eCalculated up to the last measured concentration

k_{el} was done with the last four data points (2 h to 10 h). Metronidazole also caused a shorter imatinib elimination half-life, a 17% increase in oral clearance (Cl/F) and a 21% increase in the apparent volume of distribution at steady state (V_{ss} /F). However, the mean residence time (MRT) remained unchanged between the two groups (Table 1).

Coadministration of metronidazole had a greater effect on imatinib tissue distribution (Table 2) and led to higher concentrations compared to the control group, which had several concentrations BLOQ in brain and liver (Figure 2). The T_{max} in liver and kidney remained unchanged; C_{max} was similar in liver and it was 1.7-fold higher in kidney, although the difference was not statistically significant (Mann–Whitney U test), probably due to variability in the study group. The $t_{1/2}$ was 1.9 and 2.5-fold greater in liver and kidney, respectively, in the study group. The MRT was also greater (1.9- and 1.4-fold for liver and kidney, respectively). Metronidazole coadministration resulted in a significant ($P < 0.001$) increase in $AUC_{0 \rightarrow \infty}$ in liver (1.7-fold) and kidney (2.1-fold).

The brain disposition profile is shown in Figure 2 (panel C) and a summary of the pharmacokinetic parameters is given in Table 2. Imatinib could not be quantified in most of the samples of the control group, as they were BLOQ. There was a large increase in imatinib brain uptake when metronidazole was given concurrently. In the study group, a peak was noticed very early ($T_{max} = 2$ min) that was 3.9-fold higher than the control but was not statistically significant. The concentration declined at 4 h and then rose to a second peak at 10 h, which was verified on repetition of the 6-h and 10-h time points. Because of the shape of the profile, it was not possible to identify a terminal slope in brain, thus exposure and MRT were calculated up to the last measured concentration. Metronidazole coadministration resulted in a 56-fold increase in $AUC_{0 \rightarrow t_{last}}$ and a 43% $MRT_{0 \rightarrow t_{last}}$ increase in the study group (Table 2).

Discussion

Pharmacokinetic profile in plasma

Contrary to the expected increase in exposure due to metronidazole inhibition of CYP3A4 and CYP2C9, a reduction of imatinib $AUC_{0 \rightarrow \infty}$ and C_{max} were observed but did not reach statistical significance. Lower imatinib AUC was observed after paracetamol coadministration.^[24] In addition, metronida-

zole also caused lower mycophenolic acid AUC due to lower enterohepatic recycling.^[27] Reduction of exposure may be due to higher plasma free fraction, which would lead to higher Cl and V_{ss} ^[9] as well as lower bioavailability. Several factors, including intestinal complexation reactions, enhanced gastrointestinal tract and first-pass metabolism or inhibition of the absorption,^[1] can lead to poor absorption. However, it is not likely that these processes affected imatinib bioavailability as the drugs were administered separately. Induction of metabolism may require multiple doses and no observations of active transport have been reported for metronidazole or imatinib. Imatinib is a quadrivalent basic drug, with pKa of 1.52–8.07 and freely soluble at pH 5.5.^[5] Metronidazole is also a weak base, with pKa = 2.6.^[28] Based on their pKa and the gastrointestinal tract pH, both drugs should be soluble, which would not lead to lower absorption.

Metronidazole affected the rate of absorption. The shorter T_{max} in the study group may reflect faster gastric emptying or inhibition of efflux pumps in the intestinal wall. Metronidazole has not been found to alter gastric emptying. However, it seems to be a P-gp inhibitor,^[21] although it has yet to be studied in a conclusive manner. Inhibition of intestinal wall P-gp would result in faster absorption^[29] and shorter T_{max} , as seen in the study group.

A second peak occurred in the study group at 4 h, but not in the control group (Figure 1). The second peak is likely due to enterohepatic recycling^[6] following excretion in the bile as glucuronide conjugate.^[5] This has been observed in monkeys^[7] but not in mice.^[9] Metronidazole may inhibit cytochrome P450 mediated metabolism, leading to higher glucuronide conjugate excretion in the intestine. In addition, excretion of metronidazole in the bile has been shown in rats^[17] and humans,^[30] and could inhibit P-gp in the ileum and distal colon and enhance P-gp substrate absorption. Microbial deconjugation of imatinib glucuronides to parent drug may occur in the intestine^[31] because conjugates present in plasma and urine are not detected in faeces.^[6] This imatinib reconversion may further contribute to enterohepatic recirculation. These features, together with a small intestine transit time of 4–5 h in mice and intestinal P-gp inhibition, may result in a relevant second imatinib peak, as observed in the study group. Complexation with bile acids, the presence of an absorption window or changes in pH may be ruled out, as no second peak was observed in the control group.

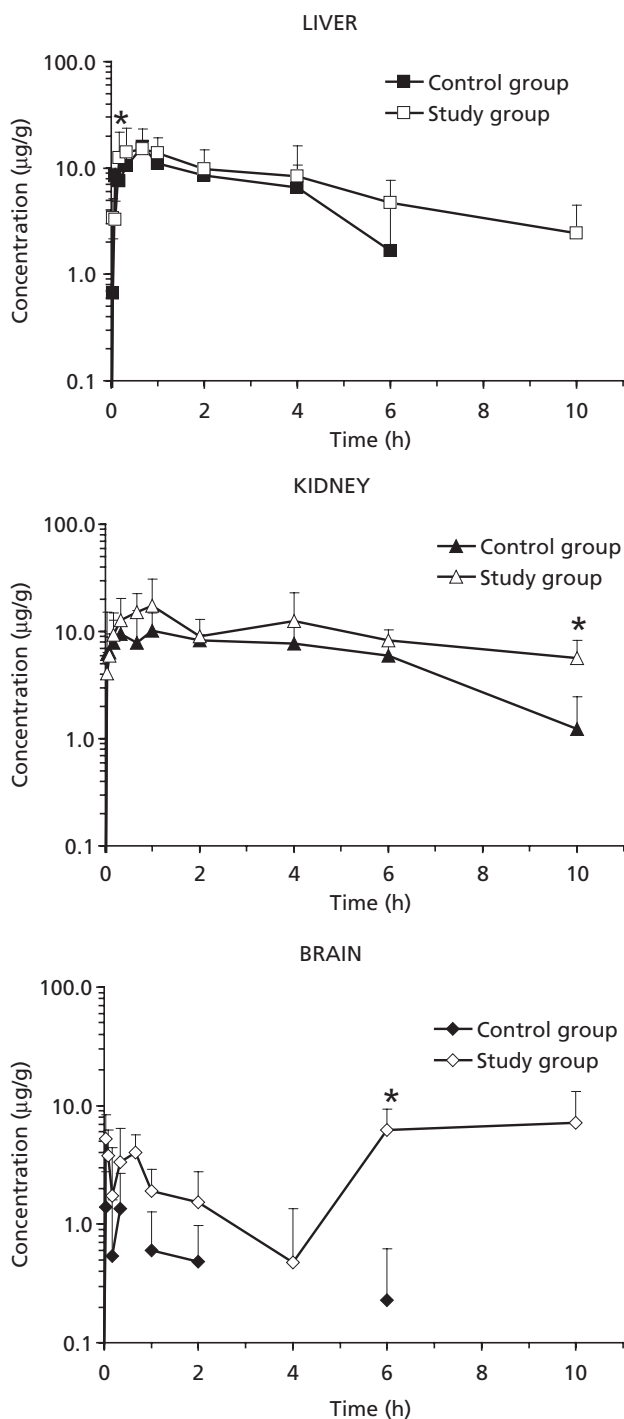


Figure 2 Pharmacokinetic profile of imatinib in tissues after oral administration of 50 mg/kg (control group; $n = 4$ per time point) or co-administered with 40 mg/kg oral metronidazole (study group; $n = 4$ per time point). Data represent mean \pm SD. *Concentrations that are statistically different based on Mann–Whitney U test. The test was not applied when the concentration was zero in that time point (e.g. brain and liver in the control group).

Metronidazole also affects the elimination of imatinib. Metronidazole has shown inhibitory effects on CYP3A4 and CYP2C9, leading to increased exposure of quinidine,^[20] tacrolimus^[21] and phenytoin.^[22] However, we observed higher k_{el} and shorter $t_{1/2}$ (Table 1). The higher k_{el} is not likely to be due to higher imatinib plasma free fraction caused by metronidazole, which has low protein binding.^[16] Rather, it may be due to an increase in tissue uptake and volume of distribution (Table 2), which may result in higher clearance (equation 1) and lower exposure (equation 2):

$$Cl = k_{el} \times V_{ss} \quad \text{Equation 1}$$

$$AUC = \frac{F \times D}{Cl} = \frac{F \times D}{k_{el} \times V_{ss}} \quad \text{Equation 2}$$

In addition to higher k_{el} , there is a large increase in the volume of distribution, evidenced by the large tissue exposure ($P < 0.001$) in brain, liver and kidney (Table 2). However, according to equation 2, in order for the AUC to remain only slightly affected, F should increase. This increase is consistent with metronidazole inhibition of intestinal P-gp, hepatic metabolism and possibly enhanced enterohepatic recycling. In the study group, there were almost parallel 17% and 20% increases in Cl/F and V_{ss}/F , respectively, which may suggest that Cl and V_{ss} are affected in similar ways. Furthermore, the changes in k_{el} and $t_{1/2}$ may have a marginal effect in comparison to the increased F and the greater tissue penetration. Further studies including metabolite kinetics would clarify the effects of V_{ss} , F and k_{el} on the AUC.

Effect of metronidazole on imatinib penetration to brain

The brain penetration of imatinib is of special interest. In-vitro studies have shown that glioma and glioblastoma cell lines are sensitive to imatinib^[12,13] but animal studies do not show the expected activity,^[14] probably because of limited brain penetration^[15] caused by P-gp and Bcrp1 efflux transporters present in the BBB.^[11] However, concurrent administration with P-gp substrates or inhibitors produces enhanced brain delivery.^[15]

Imatinib's pharmacokinetic profile in the brain after co-administration with metronidazole shows a fast uptake, which is consistent with the high blood perfusion rate in brain of 2.5 ml/min.^[32] After the C_{max} in plasma, the concentration of imatinib drops until 2 h and rises again at 4 h to give a second peak. However, the imatinib concentration in brain declines further until the 4-h time point, suggesting that brain uptake of imatinib is not taking place. Metronidazole has an elimination half-life of 1.2 h in female mice,^[19] which would lead to low plasma concentrations, unable to affect the BBB, thus preventing further brain uptake of imatinib even when imatinib plasma concentration is high (second peak). The brain imatinib concentration increases again at the 6- and 10-h time points, probably following reabsorption of metronidazole, which would inhibit the efflux transporters in the BBB to allow imatinib to redistribute to the brain. This second uptake phase leads to a greater brain-to-plasma AUC_{0-10h} ratio, which was only 4% in the control group versus 2.3-fold in the study group (Figure 3). Similarly, the study group had a longer MRT_{0-10h} , which may enhance its efficacy.

Further pharmacokinetic parameters – k_{el} , $t_{1/2}$ and extrapolated AUC – could not be determined, as it was not possible to identify a clear terminal slope (Table 2).

Distribution of imatinib to liver and kidney

Imatinib pharmacokinetics in liver and kidney (Figure 2) showed a fast uptake, probably related to their high blood perfusion rate (1.8 ml/min and 1.3 ml/min for liver and kidney, respectively).^[33] In liver and kidney, C_{max} and T_{max} were similar and did not show statistical differences between the control and study groups. After the T_{max} , imatinib concentration declined at a slower rate than in the control group. This led to longer $t_{1/2}$ and MRT and greater $AUC_{0-\infty}$ ($P \leq 0.001$) than in the study group, consistent with higher V_{ss}/F (Table 2).

The liver eliminates imatinib through microsomal oxidation followed by glucuronide conjugation and excretion of the conjugated metabolites through bile,^[6] which may be mediated by P-gp and other efflux transporters. Inhibition of metabolism and excretion could result in hepatic accumulation of imatinib, its metabolites and their conjugated forms. This is evidenced by the 1.7-fold MRT increase and the tissue-to-plasma $AUC_{0-\infty}$ ratio, which increased from 2.29 ± 0.53

(control group) to 4.53 ± 1.27 (study group) (Figure 3). In the kidney, P-gp secretes xenobiotics into the tubular filtrate before it is excreted in urine,^[29] and its inhibition would cause lower imatinib renal excretion and higher retention in the kidney. After metronidazole coadministration, the kidney imatinib $AUC_{0-\infty}$ increased 2.1-fold and the MRT increased by 39% with reference to the control group. Moreover, the kidney-to-plasma $AUC_{0-\infty}$ ratio increased from 3.04 ± 0.54 (control group) to 7.57 ± 1.98 (study group), $P < 0.001$ (Figure 3). Metronidazole’s effect on both elimination pathways seems to result in higher retention of imatinib in the liver compared to kidney, probably due to the larger contribution of the biliary–faecal route to imatinib elimination.^[6]

Clinical translatability

The clinical significance of the metronidazole–imatinib interaction is potentially important. Metronidazole inhibition of P-gp in the BBB could increase brain drug uptake, improving the treatment of glioma and glioblastoma,^[2] which are currently jeopardised by the low brain penetration.^[5] Synergism between hydroxyurea and imatinib was observed *in vitro*,^[34] but clinical trials using imatinib coadministered with hydroxyurea were disappointing and no benefit was observed in patients with glioblastoma^[35] or glioma.^[36] Unlike hydroxyurea, metronidazole and primaquine have shown enhanced imatinib brain penetration in mice.^[15]

However, increased tissue concentrations may cause changes in liver and renal function. Paracetamol, a pain-management drug used by cancer patients, affects cancer drugs’ toxicity patterns.^[37,38] Unfortunately, our study show that it is difficult to anticipate tissue concentrations based on plasma concentration data (Figure 4). Brain–plasma correlation was null (control $r^2 = 0.0009$; study group $r^2 = 0.1194$) and the kidney–plasma correlation was also very low (control $r^2 = 0.2088$; study group $r^2 = 0.3038$). The liver showed better correlation, consistent with previous studies,^[9] but it worsened on coadministration with metronidazole ($r^2 = 0.8390$ versus $r^2 = 0.4893$, respectively). This probably indicates disruption in the absorption and the liver-mediated elimination mechanisms (Figure 4).

Finally, a blood trough concentration higher than $1 \mu\text{mol/l}$ is needed to achieve desirable effects.^[39] This study also signals a potential loss of efficacy due to reduced imatinib plasma concentration. At the same time, escalation of the

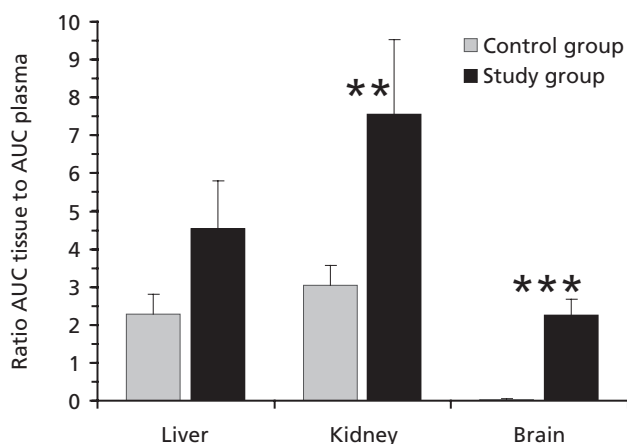


Figure 3 Imatinib $AUC_{0-\infty}$ tissue-to-plasma ratio after administration of 50 mg/kg imatinib alone (control group, $n = 4$ per time point) or coadministered with metronidazole 40 mg/kg (study group, $n = 4$ per time point). The ratio for brain was done using the AUC_{0-t} last in brain and plasma. Based on Bailer’s method: $**P < 0.01$, $***P < 0.001$.

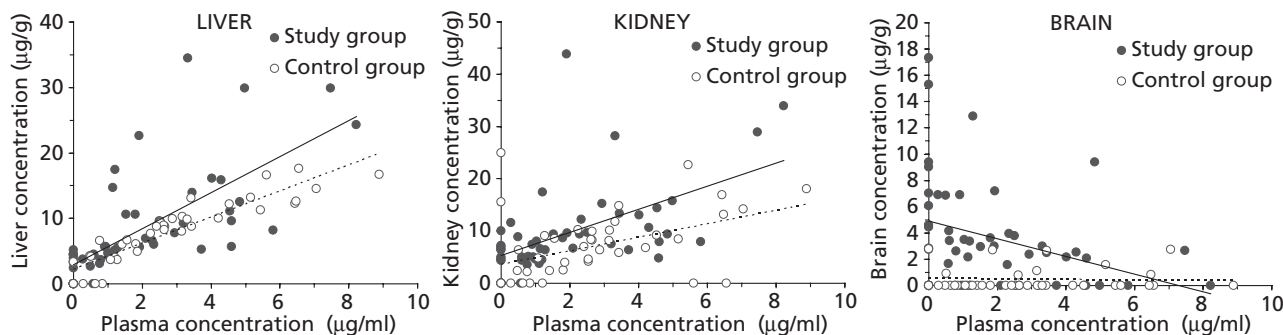


Figure 4 Correlations between concentration of imatinib in tissues and plasma after oral administration to mice in the control group and the study group. Data are the concentration in plasma and tissue for each animal.

imatinib dose up to equivalent trough levels may provide larger tissue distribution, which is beneficial for brain and renal tumours.

Conclusions

Unlike other drug interactions with imatinib that aim to improve brain-tumour treatment via a pharmacodynamic synergism, metronidazole increases imatinib brain concentration via a pharmacokinetic interaction. Although further pharmacokinetic studies are needed to evaluate the effect of metronidazole on imatinib efficacy against brain tumours, this approach could be an innovative way to address the poor therapeutic outcomes of certain brain tumours.

However, care must be taken to ensure that renal and hepatic functions are not affected on coadministration with metronidazole or other drugs that may enhance tissue distribution. It is suggested that liver and renal functions be monitored accordingly.

Declaration

Conflict of interest

The author(s) declare(s) that they have no conflicts of interest to disclose.

Funding

The authors would like to thank the International Medical University for financial support: grant # B105-Res(05)2008.

References

- Scripture CD, Figg WD. Drug interactions in cancer therapy. *Nat Rev Cancer* 2006; 6: 546–558.
- Buchdunger E *et al.* Pharmacology of imatinib (STI571). *Eur J Cancer* 2002; 38(Suppl): S28–S36.
- Castillo M *et al.* C-KIT expression in sarcomatoid renal cell carcinoma: potential therapy with imatinib. *J Urol* 2004; 171: 2176–2180.
- Wen PY *et al.* Phase I/II study of imatinib mesylate for recurrent malignant gliomas: North American Brain Tumor Consortium study 99-08. *Clin Cancer Res* 2006; 12: 4899–4907.
- Peng B *et al.* Clinical pharmacokinetics of imatinib. *Clin Pharmacokin* 2005; 44: 879–894.
- Gschwind HP *et al.* Metabolism and disposition of imatinib in healthy volunteers. *Drug Metab Dispos* 2005; 33: 1503–1512.
- Neville K *et al.* Plasma and cerebrospinal fluid pharmacokinetics of imatinib after administration to nonhuman primates. *Clin Cancer Res* 2004; 10: 2525–2529.
- Teoh M *et al.* HPLC analysis of imatinib in plasma and tissues after multiple oral dose administration to mice. *Pak J Pharm Sci* 2010; 23: 35–41.
- Teoh M *et al.* Pharmacokinetics, tissue distribution and bioavailability of imatinib in mice after administration of a single oral and an intravenous bolus dose. *Lat Am J Pharm* 2010; 29: 428–435.
- Altintas A *et al.* Central nervous system blastic crisis in chronic myeloid leukemia on imatinib mesylate therapy: a case report. *J Neurooncol* 2007; 84: 103–105.
- Bihorel S *et al.* Scherrmann. Influence of breast cancer resistance protein (Abcg2) and p-glycoprotein (Abcb1a) on the transport of imatinib mesylate (Gleevec) across the mouse blood-brain barrier. *J Neurochem* 2007; 102: 1749–1755.
- Baruchel S *et al.* A Canadian paediatric brain tumor consortium (CPBTC) phase II molecularly targeted study of imatinib in recurrent and refractory paediatric central nervous system tumours. *Eur J Cancer* 2009; 45: 2236–2238.
- Wen PY *et al.* Phase II study of imatinib mesylate for recurrent meningiomas. *Neuro-oncology* 2009; 11: 853–860.
- Wolff NC *et al.* The CNS is a sanctuary for leukemic cells in mice receiving imatinib mesylate for Bcr/Abl-induced leukemia. *Blood* 2003; 101: 5010–5013.
- Soo GW *et al.* Differential effects of ketoconazole and primaquine on the pharmacokinetics and tissue distribution of imatinib in mice. *Anti-Cancer Drugs* 2010; 21: 695–703.
- Schwartz DE, Jeunet F. Comparative pharmacokinetic studies of ornidazole and metronidazole in man. *Chemotherapy* 1976; 22: 19–29.
- Tsai TH, Chen YF. Pharmacokinetics of metronidazole in rat blood, brain and bile studied by microdialysis coupled to microbore liquid chromatography. *J Chromatogr A* 2003; 987: 277–282.
- Jensen JC, Gugler R. Single- and multiple-dose metronidazole kinetics. *Clin Pharmacol Ther* 1983; 34: 481–487.
- Bersani C *et al.* PEG-metronidazole conjugates: synthesis, in vitro and in vivo properties. *Il Farmaco* 2005; 60: 783–788.
- Cooke CE *et al.* Possible pharmacokinetic interaction with quinidine: ciprofloxacin or metronidazole? *Ann Pharmacother* 1996; 30: 364–366.
- Page RL *et al.* Potential elevation of tacrolimus trough concentrations with concomitant metronidazole therapy. *Ann Pharmacother* 2005; 39: 1109–1113.
- Blyden GT *et al.* Metronidazole impairs clearance of phenytoin but not of alprazolam or lorazepam. *J Clin Pharmacol* 1988; 28: 240–245.
- Roedler R *et al.* Does metronidazole interact with cyp3a substrates by inhibiting their metabolism through this metabolic pathway? Or should other mechanisms be considered? *Ann Pharmacother* 2007; 41: 653–658.
- Nassar I *et al.* Reduced exposure of imatinib after coadministration with acetaminophen to mice. *Indian J Pharmacol* 2009; 41: 167–172.
- Bailer AJ. Testing for the equality of area under the curves when using destructive measurement techniques. *J Pharmacokin Biopharm* 1988; 16: 303–309.
- Yuan J. Estimation of variance for AUC in animal studies. *J Pharm Sci* 1993; 82: 761–763.
- Naderer OJ *et al.* The influence of norfloxacin and metronidazole on the disposition of mycophenolate mofetil. *J Clin Pharmacol* 2005; 45: 219–226.
- Cho MJ *et al.* Metronidazole phosphate – a water-soluble prodrug for parenteral solutions of metronidazole. *J Pharm Sci* 1982; 71: 410–414.
- Matheny CJ *et al.* Pharmacokinetic and pharmacodynamic implications of p-glycoprotein modulation. *Pharmacotherapy* 2001; 21: 778–796.
- Nielsen ML, Justesen T. Excretion of metronidazole in human bile. Investigations of hepatic bile, common duct bile, and gallbladder bile. *Scand J Gastroenterol* 1977; 12: 1003–1008.
- Chourasia MK, Jain SK. Pharmaceutical approaches to colon targeted drug delivery systems. *J Pharm Pharmaceut Sci* 2003; 6: 33–66.
- Cattelotte J *et al.* In situ mouse carotid perfusion model: glucose and cholesterol transport in the eye and brain. *J Cereb Blood Flow Metab* 2008; 28: 1449–1459.

33. Davies B, Morris T. Physiological parameters in laboratory animals and humans. *Pharm Res* 1993; 10: 1093–1095.
34. Ren H *et al.* Differential effect of imatinib and synergism of combination treatment with chemotherapeutic agents in malignant glioma cells. *Basic Clin Pharmacol Toxicol* 2009; 104: 241–252.
35. Reardon DA *et al.* Multicentre phase II studies evaluating imatinib plus hydroxyurea in patients with progressive glioblastoma. *Br J Cancer* 2009; 101: 1995–2004.
36. Desjardins A *et al.* Phase II study of imatinib mesylate and hydroxyurea for recurrent grade III malignant gliomas. *J Neurooncol* 2007; 83: 53–60.
37. Nassar I *et al.* Histopathological study of the hepatic and renal toxicity associated to the coadministration of imatinib and acetaminophen in a preclinical mouse model. *Malays J Pathol* 2010; 32: 1–11.
38. Lim AYL *et al.* Histopathology and biochemistry analysis of the interaction between sunitinib and paracetamol in mice. *BMC Pharmacol* 2010; 10: 14 (1–17).
39. Picard S *et al.* Trough imatinib plasma levels are associated with both cytogenetic and molecular responses to standard-dose imatinib in chronic myeloid leukemia. *Blood* 2007; 109: 3496–3499.